# Photoabsorption $K$ Edge of Shock Compressed Aluminum

François Perrot[1] and M. W. C. Dharma-wardana[2]

[1]Centre d'Etudes de Limeil-Valenton, 94195-Villeneuve St. Georges-Cedex, France
[2]National Research Council of Canada, Ottawa, Canada K1A 0R6

The $K$-edge shift and the absorption profile of aluminum along the shock Hugoniot have been calculated using density functional methods taking account of finite temperature effects, lattice melting, and liquid structure. Our first principles calculation is in good accord with available experiments.

Recent advances in experimental techniques provide a probe for matter at extreme conditions of temperature and pressure [1,2]. Such studies are important in plasma physics, geophysics, astrophysics, and also as a testing ground of basic physics. Although thermodynamic properties (e.g., along the shock Hugoniot) are well established [3], the study of spectral properties, transport properties, etc., are only just becoming available [4,5]. The positions of spectral *lines*, unlike positions [6] of *levels*, are obtainable by experiment. Line shifts are a complex measure of many-body effects due to ions, electrons, and photons. The usual theory of the line shape and shift in low-density systems [7] is not suitable for dense plasmas where both electron-ion and ion-ion interactions are important. There have been suggestions [8] that energy levels *remain unshifted* for a large range of densities. Also, a recent theory [9] uses statistically weighted *unshifted* energy levels to construct partition functions and related properties. Hence, comparison of experiment with first principles theory is needed even though experiments on extreme states of matter are difficult.

A particularly challenging case is the x-ray edge problem [10] where density functional theory [11,12] (DFT) at $T=0$ K has [13] successfully complemented the Mahan-Nozières-DeDominicis-Combescot (MNDC) approaches [10]. MNDC deals with the $T=0$ K edge profile but the position of the edge, $v_T$, is assumed known. That is, although shifts and shapes are connected by the usual dispersion relations, MNDC ignore the *edge-shift* calculation. Here we present a $T \neq 0$ K calculation of the $K$-edge shift and profile of $Al^{3+}$ along the shock Hugoniot using DFT, and compare with experimental results [5].

In Ref. [5] the $K$-edge shift was treated as a sum of *level* contributions. But the x-ray edge is complicated by final state interactions (FI) of the Fermi sea, "orthogonality catastrophe" [14], band structure, phonons, screening, and lifetime effects of the core hole. Only some of these issues (not handled in Ref. [5]) are handled by MNDC. In a shock compressed system (e.g., $Al^{3+}$ along the shock Hugoniot [15]) the FI involve *both* electrons and ions which may be in a fluid phase. The shock heats electrons and ions and a distribution of electron and ion configurations becomes relevant.

The FI and orthogonality catastrophe are difficult to treat in the dynamical theory using collision operators or Green functions defined in an energy *level* basis. In DFT *total* energies of the $N$ and $N-1$ electron system are considered instead of energy levels. Thus the line position is calculated as the difference in "ground state" energies of the final state $F$ and the initial state $I$. The $F$ is not an exact ground state, but a "legislated" ground state having a core hole in the $1s$ level of the $Al^{4+}$ system and causing final state interactions. The calculation of ground state energies (or free energies at finite temperature) includes final state electron interactions. Standard models of exchange and correlation at finite temperature [16] will be used in this study. In fact recent work [17] seems to suggest that the edge *profile* problem can be treated within a more conventional framework, without recourse to the heavier MNDC approaches.

Consider an $Al^{3+}$ ion at mean free electron density $\bar{n}$ and ion density $\bar{\rho}$, with ionic charge $\bar{z}=3$ for Al ions. Let the electron- and ion-density profiles around an $Al^{z+}$ ion at the origin be $n(r)$ and $\rho(r)$. For compressions $\kappa = \bar{\rho}/\rho_0$ up to 4 times the normal density $\rho_0$ (with $\rho_0 = 2.70$ gcm$^{-3}$ at normal temperature and pressure), only $Al^{3+}$ ions occur. Thus $z=\bar{z}=3$ for the field ions. The initial state will be denoted by $z_I = z_3$, $n_I(r) = n_3(r)$, $\rho_I(r) = \rho(r)$, while the final state is $z_F = z+1 = 4$ and will be denoted by $z_4, n_4(r), \rho(r)$ with an electron added to the sea of electrons of average density $\bar{n}$. The field-ion charge $z_3$ remains unchanged. The field-ion distribution is $\rho(r)$ for both $I$ and $F$ since ion-dynamical effects are negligible [18].

The temperature along the Al shock Hugoniot can be deduced [15] using the equation of state. The ion lattice melts at approximately 0.25 eV. Aluminum is a "simple metal" or a "simple plasma" [19] in the sense that *weak* electron-ion pseudopotentials $V^{ei}$ can be constructed such that results using $V^{ei}$ agree with the full nonlinear DFT calculations to high accuracy. This implies that the DFT calculation using coupled equations [12] for electron and ion profiles can be replaced by a neutral pseudoatom (NPA) calculation where the electron problem is decoupled from the ion problem. The construction of $V^{ei}$ used by us is as follows. Let $\Delta n(q)$ be the Fourier component of the full (nonlinear) free-electron density displacement $\Delta n(r) = n(r) - \bar{n}$ around an ion in the uniform electron gas (EG) of density $\bar{n}$ and temperature $T$. Then we *define* $V^{ei}(q)$ by the relation $\Delta n(r) = -V^{ei}(q)\chi(q,\bar{n},T)$

where $\chi(q,\bar{n},T)$ is the full EG response function. This absorbs the nonlinearities into $V^{ei}$ entirely. This is adequate for Al, although not in general. In the NPA procedure a uniform positive background (jellium) with a spherical cavity $v(r)$ of radius $r_{WS} = (3\bar{n}/4\pi z)^{1/3}$ is placed around the central ion and perturbation theory (PT) is used to correct for the cavity. The positive charge removed to form the cavity is just the charge $+z$ at the origin. The "central ion+cavity" is the NPA having a zero Friedel sum, i.e., an ideal weak scatterer for which PT is applicable. When such a jellium with a cavity is employed the pseudopotential [19]

$$V^{ei}_{z3}(q) = \Delta n_z(q)/\chi(q) - (4\pi/q^2)v_z(q) \qquad (1)$$

is used, with $z = 3$ or 4 for $I$ or $F$. Here we use perturbation theory for treating the ion distribution after verifying that the PT calculations agree with the full nonlinear DFT calculation for several test densities.

First consider the $T = 0$ K case for a system of $N$ ions. The total energy $E_3$ for the $Al^{3+}$ system is given by the NPA energy of the central ion at the origin plus the PT contribution $\Delta E^{ei}_3$ per ion of the $N - 1$ field ions. Thus

$$E_3 = E^e_3 + E^{ei}_3 + E^i_3 + (N - 1)\Delta E^{ei}_3 . \qquad (2)$$

The electron, electron-ion, and ion contributions are identified by the superscripts. The $E^e_3$ contains the uniform EG energy and a correction from the "band-structure zero" of energy

$$E^e_3 = N z_3 \varepsilon(\bar{n}) + \frac{N}{2}\bar{n}z_3\left[\frac{1}{\chi_0(0)} - \kappa(0)\right] . \qquad (3)$$

Here $\chi_0(0)$ is the $q \to 0$ limit of the noninteracting EG response; $\kappa(0) = d\mu_{xc}(\bar{n})/d\bar{n}$ is related to the local field (compressibility) correction of $\chi(q \to 0)$. The term $E^{ei}_3$ arises from the central ion+cavity and is

$$E^{ei}_3 = \Delta E_3 + \int d\mathbf{r}(\bar{n} - v_3)Y_3 + \int d\mathbf{r}\frac{1}{2}v_3\frac{1}{r} * (v_3 - m_3) . \qquad (4)$$

Here $\Delta E_3$ is the embedding energy of the $Al^{3+}$ ion in the jellium with the cavity $v_3$ (of charge $z_3$). This is evaluated from the phase shifts of the Kohn-Sham scattering states using Fumi's theorem and the bound state energies. The remaining terms are cavity corrections, with

$$Y_3 \equiv -\frac{z_3}{r} + \frac{1}{r} * \{v_3 + \Delta n_3\} .$$

Here $\Delta n_3(r)$ is the displaced charge of the continuum electrons around the $Al^{3+}$ neutral pseudoatom and integrates to zero. The "$*$" defines the convolution product $u*v = \int u(\mathbf{s})v(\mathbf{r} - \mathbf{s})d\mathbf{s}$. Finally, in the last term of Eq. (4), $m_3(r)$ is calculated from $m_3(q) = -(4\pi/q^2)v_3(q) \times \chi(q)$, i.e., a linear response to the cavity. Thus $E^{ei}_3$ accounts for the complete structure of the ion in its medium, and the nonlinear response of the electrons to the ion potential. Finally, the ionic energy $E^i_z$ can be written as

$$E^i_3 = \frac{N}{2}\sum_{i \neq 0} V_{33}(R_i) = \bar{\rho}\int d\mathbf{r}\, V_{33}(r)g(r) , \qquad (5a)$$

$$V_{z3}(r) = \frac{(zz_3)}{r} + \int d\mathbf{q}\,|V^{ei}_{z3}(q)|^2\chi(q)\exp(-i\mathbf{q}\cdot\mathbf{r}) . \qquad (5b)$$

Here $z = 3$ for $I$, the initial state. $V_{33}(r)$ is the ion-pair potential (see Fig. 1) and $g(r)$ is the ion-pair correlation function. At $T = 0$ this reduces to a lattice sum. $V^{ei}_{z3}(q)$ is defined in Eq. (1). The PT correction to the electron-ion interaction of the $N - 1$ field ions, denoted by $\Delta E^{ei}_3$ is

$$\Delta E^{ei}_3 = (2V)^{-1}\sum_q |V^{ei}_{33}(q)|^2\chi(q) . \qquad (6)$$

Similarly the total energy of the final state $F$ is ($Al^{4+}$ ion at the origin)

$$E_4 = E^e_4 + E^{ei}_4 + E^i_4 + (N - 1)\Delta E^{ei}_3 + E_{photo} , \qquad (7)$$

$$E_{photo} = E_F + \mu_{xc} , \qquad (8)$$

$$E^e_4 = E^e_3 + (z_4 - z_3)\bar{n}[\chi_0(0)^{-1} - \kappa(0)] ,$$

$$E^i_4 = \left(\frac{N}{2} - 1\right)\sum_{i \neq 0}V_{33}(R_i) + \sum_{i \neq 0}V_{43}(R_i) .$$

$E^{ei}_4$ is similar to $E^{ei}_3$ with the appropriate quantities. $\Delta E^{ei}_4$ is identical to $\Delta E^{ei}_3$. Here $E_{photo}$ is the energy of the photoionized electron placed at $E_F$, plus an exchange-correlation correction $\mu_{xc}$. The term $E^e_4$ has a local field (band-structure zero) correction from the change $z_3 \to z_4$ at the origin. The ionic energy $E^i_4$ contains $V_{43}(R_i)$, Eq. (5b), viz., the interaction (Fig. 1) between the $Al^{4+}$ ion at the origin and a field ion $Al^{3+}$ at $R_i$. The embedding energy of the $Al^{4+}$ ion is $\Delta E_4$ and is contained in $E^{ei}_4$. This is calculated from the Kohn-Sham phase shifts and bound state energies.

Given the initial and final total energies $E_3$ and $E_4$ at $T = 0$ K, the transition energy is

$$hv = E_4 - E_3 . \qquad (9)$$

We ignore phonon effects [18] since phonon energies are negligible compared to $hv$. Our calculated position of the
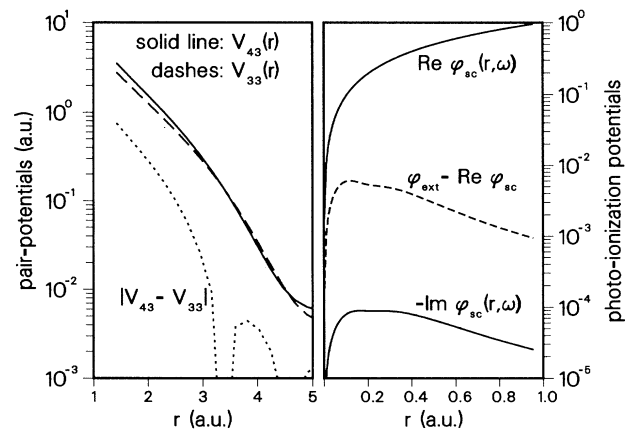


FIG. 1. Left: The initial and final state ion-ion pair potentials $V_{33}(r)$ and $V_{43}(r)$ at compression 2. See Eq. (5b). The ionic core radius is $\approx 1.4$ a.u. Right: The external (photon) potential $\phi_{ext}(r,\omega)$ is modified to $\phi_{sc}(r,\omega)$ due to the photoresponse of the atom [21]. The mean radius of the $1s$ level is 0.120 a.u.

$Al^{3+}$ $K$ edge at normal density (i.e., $\kappa = 1.0$) and $T = 0$ K is 1560.2 eV, in close agreement with the experimental value [20] of 1560 eV.

At $T \neq 0$ K DFT minimizes the Helmholtz free-energy $\mathcal{F}$, while the transition involves the internal energy difference $E_4 - E_3$. Unlike at $T = 0$ K, there is a thermal ensemble of configurations and the "$K$ edge" is the "observable" onset of absorption. In effect, at $T \neq 0$ K there are holes at every energy $\varepsilon$ in the Fermi sea with a probability $1 - f(\varepsilon/T)$ where $f(\varepsilon/T)$ is the Fermi function. The energy $E_F$ in Eq. (8) has to be replaced by $\varepsilon$, and the $T \neq 0$ K transition energy is

$$h\nu = \langle E_4 \rangle - \langle E_3 \rangle + \varepsilon + \frac{\partial}{\partial \beta} (\beta \mu_{xc}) ; \qquad (10)$$

here, e.g.,

$$\langle E_3 \rangle = \Delta E_3 + 4\pi \bar{\rho} \int g(r) \frac{\partial}{\partial \beta} \{\beta V_{33}(r)\} r^2 dr$$
$$+ \frac{\partial}{\partial \beta} \beta(C + D), \qquad (11)$$

where $C$ and $D$ refer to the last two terms of Eq. (4) at $T \neq 0$ K. Here $\Delta E_3$ and similarly $\Delta E_4$ are the $T \neq 0$ K embedding energies of the $T \neq 0$ K Kohn-Sham calculation. The other terms evaluated by the $T \neq 0$ K DFT code are free energies and are converted to internal energies in the ensemble averaging via the operation $(\partial/\partial \beta)(\beta \cdots)$ applied to them. For $k_B T > 0.25$ eV the ions are in a liquid state and the lattice sums become an averaging over the ion-pair correlation function $g(R)$ calculated using the modified hyper netted-chain equation (containing a bridge term) for the pair-interaction $V_{33}(R)$.

Equation (10) gives the transition energy, inclusive of final state interactions, etc., when an electron goes from the $1s$ level in $Al^{3+}$ of the compressed material to a continuum energy $\varepsilon$, with $\varepsilon > 0$ and it *does not define* an edge as in the $T = 0$ K case for $\varepsilon = E_F$. In an *actual experiment* the observed absorption will remain very low up to energies within $k_B T$ of the Fermi energy when the absorption will rise appreciably, giving a pseudoedge. At higher temperatures ($k_B T > E_F$) even this feature will be lost, and hence a criterion of the "onset" of the transition is needed.

The MNDC line shape is

$$I(\nu) \propto I^0(\nu) [\xi/(\nu - \nu_T)]^\alpha , \qquad (12)$$

where $I^0(\nu)$ is the profile calculated without the MNDC corrections. $\xi$ is of the order of $E_F$. The edge exponent $\alpha$ can be expressed [10] in terms of the difference in phase shifts $\Delta \delta_l = \delta_{l,F} - \delta_{l,I}$ for the $l$th partial wave at the Fermi energy. The orthogonality catastrophe acts to moderate the effects of $\alpha$. The edge exponents at $T = 0$ for several densities were calculated and $\alpha$ is of the order of 0.1. Hence we ignore the edge exponents but evaluate the profile using the correct initial and final states. Zangwill and Soven (ZS) [21] showed that the LDA-absorption profile can be very different from the true profile, due to dynamic screening of the external photon

potential $\phi_{ext}(r,t) = \mathbf{E} \cdot \mathbf{d} \cos(\omega t)$ where $\mathbf{d}$ is the dipole operator. Our experience [22] of a $T \neq 0$ K version of the ZS method is that these effects are not important for the $K$ edge. This is confirmed by calculating the ZS self-consistent photoionization potential $\phi_{sc}(r,\omega)$. The real and imaginary parts of $\phi_{sc}(r,\omega)$ for $\omega = \mu_0 - \varepsilon_{1s}$ at compression 3 are shown in Fig. 1. This provides the ZS profile $I_{zs}(\nu) = I_0(\nu) + I[\Delta \phi_{sc}(r,\omega)]$ where the last term arises from the induced photoionization potential. $I_0(\nu)$ involves the matrix element of the unmodified $\phi_{ext}(r,\omega)$ and is discussed below. The induced potential changes the profile by a small almost constant factor, i.e., $I_{zs}(\nu) \approx 0.94 I_0(\nu)$.

In calculating $I_0(\nu)$ we evaluated $\langle 1s | \mathbf{V} \cdot \mathbf{u} \exp \times (i\mathbf{q} \cdot \mathbf{r}) | k \rangle$ where $|k\rangle$ is the final state $\phi_{klm}(r) Y_{lm}(r)$, with $k^2/2 = \varepsilon$, and averaged over the angle of $\mathbf{q}$, and summed over $l,m$. The terms beyond the dipole term contributed $< 4\%$ to the profile. The final state is weighted by the thermal factor $1 - f(\varepsilon/T)$. We include no ion dynamics [18,23] but include the Auger width [20] and write

$$I(\nu) = \int_{-\infty}^{+\infty} I_0(\omega) \frac{\Gamma}{(\Gamma/2)^2 + (\omega - \nu)^2} \frac{d\omega}{2\pi} , \qquad (13)$$

where $\Gamma = 0.6$ eV. The observable edge is defined as that value of $\nu = \nu_T$ where the intensity $I_{edge}$ scaled by the maximum absorption intensity $I_{max}$ is a certain preassigned value $f$, viz.,

$$f = I_{edge}/I_{max} . \qquad (14)$$

For $f = 0.1$ and 0.05 the calculated edge shift at compression $\kappa = 1.25$ remains 0.21 eV, while at $\kappa = 2$ they are 2.98 and 3.39 eV [the ZS correction leaves Eq. (14) unaffected]. This uncertainty at higher temperatures reflects the lack of a true edge. We report our calculated
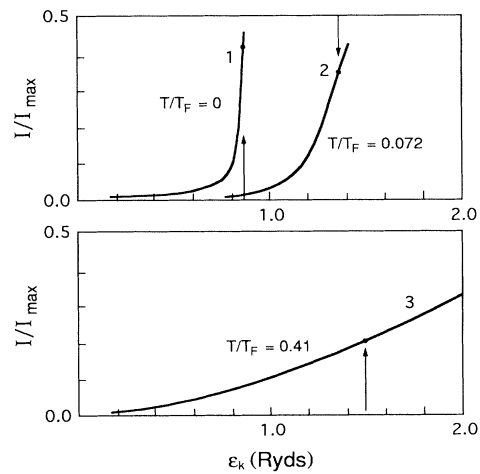


FIG. 2. The calculated edge profiles at compressions $\kappa = 1, 2,$ and 3 and $T = 0$ K, $1.55 \times 10^4$ K, and $1.15 \times 10^5$ K. Vertical arrows: chemical potential $\mu_0 = 0.86$, 1.36, and 1.50 Ry, respectively.
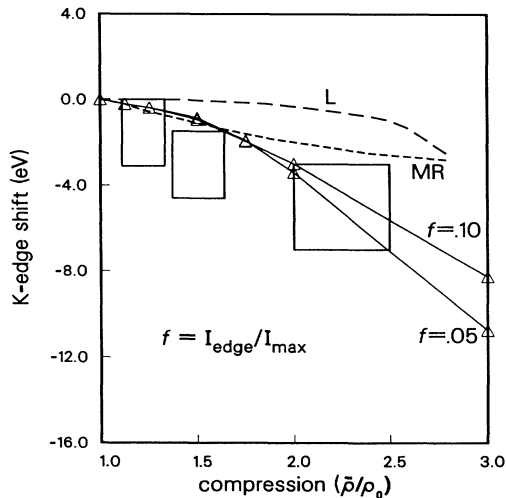
FIG. 3. The calculated and measured [5] (large boxes) $K$-edge shift along the Hugoniot as a function of compression. [L: Liberman, MR: McMahan and Ross cited in Ref. [5], present work: $f = 0.1$ and 0.05; see Eq. (14)].

absorption profiles in Fig. 2, while the shifts, calculated with $f = 0.1$ and 0.05, are shown (Fig. 3) as triangles.

Figure 2 shows the absorption profiles (scaled by $I_{max}$ which is weakly dependent on $\kappa$) for $\kappa = 1$, 2, and 3 with $T/T_F = 0$, 0.072, and 0.41, $T_F$ being $E_F/k_B$. The chemical potential $\mu_0$ at a given compression (e.g., $\kappa = 3$) depends on the accompanying increase of temperature. The shift of the absorption edge (at $f = 0.05$ and 0.1) from the $\kappa = 1$ value is plotted in Fig. 3. No profiles were calculated in Ref. [5]. Two shift calculations (MR and L) reported in Godwal et al. [5] and the experimental data [5] are also shown. The second data box straddles the phase transition. The McMahan and Ross (MR) curve is a solid state APW calculation and we agree closely with MR in the solid regime (it is not clear if MR used a $T \neq 0$ exchange-correlation correction). Liberman's (L) sophisticated code does not include $T \neq 0$ K exchange-correlation effects, liquid structure, or final state interactions except for Slater's transition state model. Our theory includes a rigorous $T \neq 0$ K analysis, final state interactions, and explicit liquid state effects via modified hypernetted-chain theory. We provide a profile calculation and a definition of a "pseudoedge." Although the experiment has a large uncertainty, the curve L and MR in the liquid range clearly underestimate the edge shift. These experimental and theoretical results suggest that energy levels and spectral lines (in this case the edge) show red shifts under compression although this lacks consensus in the plasma literature [8,24].

We thank Andrew Ng for helpful discussions and Walter Kohn for suggesting this problem to us at the Santa Cruz meeting on dense plasmas.

[1] High Intensity Laser-Matter Interactions, SPIE Proceedings, Vol. 13, edited by E. M. Campbell and H. Baldis (SPIE, Bellingham, 1988).

[2] "Laser Interactions with Atoms, Solids, and Plasmas," edited by R. M. More, NATO ASI (Plenum, New York, to be published).

[3] M. Ross, Rep. Prog. Phys. 68, 1 (1985).

[4] D. K. Bradley et al., Phys. Rev. Lett. 59, 2995 (1987); T. A. Hall et al., ibid. 60, 2034 (1988).

[5] B. K. Godwal, A. Ng, L. Da Silva, Y. T. Lee, and D. A. Liberman, Phys. Rev. A 40, 4521 (1989).

[6] M. W. C. Dharma-wardana and F. Perrot, Phys. Rev. A 45, 5883 (1992).

[7] H. R. Griem, Spectral Line Broadening in Plasmas (Academic, New York, 1974); D. Boereker et al., Phys. Rev. A 30, 2771 (1984).

[8] W. D. Kraeft, D. Kremp, K. Kiliman, and H. E. Dewitt, Phys. Rev. A 42, 2340 (1990).

[9] D. Mihalas, W. Daeppen, and D. G. Hummer, Astrophys. J. 331, 815 (1988).

[10] See, G. D. Mahan, Many-Particle Physics (Plenum, New York, 1990), Chap. 8; also C.-O. Almbladh and L. Hedin, in Handbook on Synchrotron Radiation, edited by E. Koch (North-Holland, Amsterdam, 1983), Vol. 18, p. 607.

[11] P. Hohenberg and W. Kohn, Phys. Rev. 136, B864 (1964); N. D. Mermin, Phys. Rev. 137, A1441 (1965); W. Kohn and L. J. Sham, ibid. 140, A1133 (1965).

[12] M. W. C. Dharma-wardana and F. Perrot, Phys. Rev. A 26, 2096 (1982); Strongly Coupled Plasmas, edited by F. Rogers and H. E. DeWitt (Plenum, New York, 1986), p. 275.

[13] C.O. Almbladh and U. von Barth, Phys. Rev. B 13, 3307 (1976).

[14] P. W. Anderson, Phys. Rev. Lett. 18, 1049 (1967).

[15] G. I. Kerley, Report Sandia No. 88-2291 UC-405, 1991 (unpublished).

[16] F. Perrot and M. W. C. Dharma-wardana, Phys. Rev. A 30, 2619 (1984).

[17] E. Zaremba and K. Sturm, Phys. Rev. Lett. 66, 2144 (1991).

[18] Including ion-electron coupling in the transition current-current Green function gives a shift and broadening dependent on the reciprocal of the (large) transition frequency. Hence we ignore ion-dynamical effects.

[19] F. Perrot, Phys. Rev. A 42, 4871 (1990); also J. M. Ziman, Proc. R. Soc. London 91, 701 (1967).

[20] H. Neddermeyer, Phys. Lett. 44A, 181 (1973).

[21] A. Zangwill and P. Soven, Phys. Rev. A 21, 1561 (1980); A. Zangwill and D. Liberman, J. Phys. B 17, L253 (1984).

[22] F. Grimaldi, A. Grimaldi-Lecourt, and M. W. C. Dharma-wardana, Phys. Rev. A 32, 1063 (1985).

[23] Ion configuration fluctuations (Debye-Waller effects, "ion microfields") affect the far line wing. The results do not change significantly [18].

[24] See Refs. [8,9] and also, for example, S. Goldsmith et al., Phys. Rev. A 30, 2775 (1984).